

# MEASUREMENT OF GEOACOUSTICAL PARAMETERS WITH ULTRA LOW FREQUENCY WAVES

Barbara Nicolas, Jérôme Mars, François Glangeaud, Jean-Louis Lacoume

Laboratoire des Images et Signaux, INPG  
Rue de la Houille blanche, 38402 Saint Martin d'Hères, FRANCE  
[Barbara.Nicolas@lis.inpg.fr](mailto:Barbara.Nicolas@lis.inpg.fr)

## ABSTRACT

Geoacoustical parameters estimation is a crucial issue in oceanic engineering, underwater acoustics and marine geophysics [2,3,11]. We show that these parameters can be estimated with Ultra Low Frequency waves using signal processing tools. To determine the useful processing methods or representations, a study of the propagation between an underwater source and receivers laid on the sea floor is proposed for oceanic wave guides. Processing methods adapted to this context are described : velocity correction, frequency-wave-number transform. Finally, geoacoustical parameters estimation is illustrated on three data sets recorded on displacement detectors (geophone) and pressure sensors (hydrophone) in different environments (depths and seabed characteristics).

## 1. INTRODUCTION

Ultra Low Frequency waves (1-100 Hz) are now widely used in underwater acoustic to reach information on propagation parameters (acoustic and elastic). Because ULF waves are almost non-affected by absorption during their underwater propagation, they can be used to estimate geoacoustical parameters at long-range. In this case and in shallow water, preponderant waves are guided waves, they must be taken into account during the horizontal transmission between an underwater source and receivers laid on the sea floor. To reach this information, different receivers can be used : hydrophones that recorded the pressure field or 4-components receivers named Ocean Bottom Seismometers (OBS) which provide the three components of the displacement and the pressure field.

Our objective is to show that using ULF waves in shallow water and appropriate signal processing tools, it is possible to extract physical information on geoacoustical parameters. The paper will be organized as follows: a presentation of guided waves in term of physics is made. The second part briefly present suitable methods for geoacoustical parameters estimation. And in the last part, three seismic refraction data recorded in shallow water (35, 100, 140 meters depth), recorded by OBS or hydrophones, are processed to recover geoacoustic parameters.

## 2. DESCRIPTION OF THE PROPAGATION MODES

### 2.1. General Context

Geoacoustical parameters estimation based on wave theory depends on the model of propagation in the acoustic (sea) and elastic (seabed) media. Let us consider an omnidirectional impulsive source located under the sea surface (Fig. 1). Waves arriving on the sea floor with an incident angle  $\theta_1$  inferior to the critical reflexion angle  $\theta_c$  are partially transmitted in the sea floor [7]. They do not contribute to long distance whereas totally reflected waves, guided between the sea surface and bottom, propagate in the wave guide. As a result, proposed methods to estimate geoacoustical parameters will be based on wave guide theory.

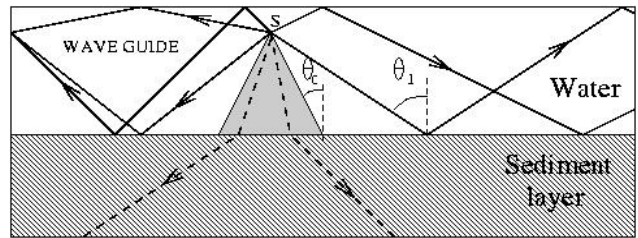


Fig. 1: Propagation approximation

### 2.2. Wave Guide

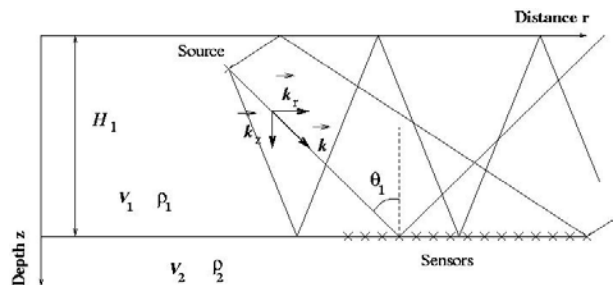


Fig. 2: Wave guide parameters

After this brief introduction, a simple model of homogeneous wave guide is presented (Fig. 2). Parameters necessary for studying the wave guide between an underwater source and receivers laid on the floor are:  $H_1$  the water depth,  $v_1$  the P-wave velocity in the water layer,  $v_2$  the P-wave velocity in the first sediment layer,  $\rho_1$  the density of the water layer and  $\rho_2$  the density of the sediment layer.  $r$  represents the horizontal distance and  $z$  the depth.  $\vec{k}$  is the

wavenumber and can be projected on distance and depth axis. As  $\vec{k}$  is perpendicular to the wavefront, it is possible to express  $k_r$  and  $k_z$  depending on the incident angle  $\theta_1$ :

$$k_z = k \cos \theta_1, k_r = k \sin \theta_1 \text{ with } k = f / V_1 \quad (2.1)$$

During the propagation path, interferences between different waves (upgoing or downgoing) appear creating guided waves [4,10]. Fig. 3 summarizes the interference principle in a homogeneous wave guide.  $R_1$  and  $R_2$  are respectively the reflexion coefficients of the air/water interface and of the water/sea-floor interface.

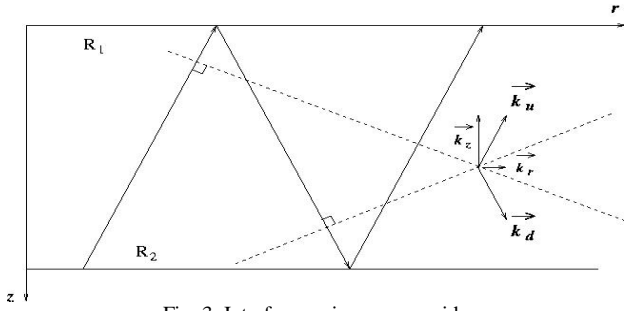


Fig. 3: Interference in a wave-guide

In order to interfere constructively, two waves fronts (which differ from two reflections at the sea surface and at the sea floor) must present a phase shift multiple of  $2\pi m$ . This condition, known as resonance condition, can be written as:

$$R_1 R_2 e^{4\pi j k_{zm} H_1} = e^{2\pi j m} \quad (2.2)$$

Using this expression, we can express the relation for the mode  $m$  between the frequency  $f_m$  and the angle of incidence  $\theta_1$  (or the horizontal wavenumber  $k_r$ ) [9,1]. Focusing on the critical angle ( $\theta_1 = \theta_c$ ), this relation allows to recover the cutoff frequency of each mode :

$$f_{cm} = \frac{(2m-1)V_1}{4H_1 \sqrt{1-(V_1/V_2)^2}} \quad (2.3)$$

## 2.2. Modes characterization

### • Characterization tool: frequency-wavenumber transform

In order to characterize propagation modes, we introduce the “frequency-wavenumber” representation, which is the square modulus of the 2D Fourier transform of a section  $p(r, z, t)$  in time  $t$  and radial distance  $r$  at a given depth  $z$  [8]. This representation, named  $f-k$  representation, is :

$$P(k_r, z, f) = \left| \iint p(r, z, t) e^{-2\pi j (ft - k_r r)} dt dr \right|^2 \quad (2.4)$$

### • Modes characterization in the $f-k$ domain

At a depth  $z_0$ , pressure field becomes :

$$p(k_r, z_0, f) = S(f) \sum_m A_m \Psi_m(z_0) \delta[k_r - k_{rm}] \quad (2.5)$$

The  $f-k$  representation of the pressure field (Fig. 4) permits the separation of the different modes [6][8]: if the incident angle is inferior to the critical angle, waves do not propagate at long range. As a result, the limit waves that can interfere in the wave guide have a wavenumber oriented in the critical angle direction. In this case,

$$k_z = f \cos \theta_1 / V_1 = f \sqrt{1 - (V_1/V_2)^2} / V_1 \quad \text{and using}$$

$$k_{rm}^2 + k_{zm}^2 = f / V_1 \quad (2.6)$$

we obtain  $k_{rm} = f / V_2$  which is a straight line passing through the cutoff frequencies. The other limit of incidence angle is when the wavenumber is oriented in the horizontal direction ( $k_{zm} = 0$ ), (2.11) becomes  $k_{rm} = f / V_1$  which is the asymptote above which modes exist in the  $f-k$  domain. Between these two straight lines, modes exist and propagate: the relation between  $f_m$  and the horizontal wavenumber  $k_r$  is represented on fig. 4.

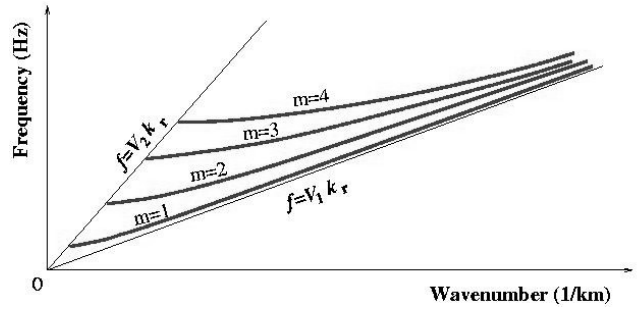


Fig. 4: Modes representation in the  $f-k$  domain

## 3. GEOACOUSTICAL PARAMETERS ESTIMATION

In this section, signal processing tools are used to estimate geoaoustical parameters: water layer velocity  $V_1$ , first sedimentary layer velocity  $V_2$ , water depth  $H_1$  [5][6][8].

### 3.1. Estimation of the water layer velocity $V_1$

Propagation in the water layer is first characterized by a direct wave recorded on receivers laid on the floor. Temporal positions of the arrivals depend on the offset between the underwater source and each receiver. To estimate  $V_1$ , from initial section in the distance-time domain  $[r, t]$ , we apply a time correction along the distance axis  $r$ . The recorded signal of each sensor is time shifted so that the direct wave impinges on all sensors at the same time. This time correction gives an estimation of the water layer velocity.

### 3.2. Estimation of the first sediment layer velocity $V_2$

To estimate  $V_2$ , we use the  $f-k$  representation on the entire section (Fig. 5), which shows different modes of propagation and allows us to use physical characterization established in the first part of this paper. After  $V_1$  velocity correction, the straight line  $f = V_2 k_r$  is shifted in  $f = V_{app2} k_r$ .  $V_{app2}$  is the apparent refracted wave velocity measured on the  $f-k$  representation and can be expressed by  $V_2^{-1} = 1/V_{app2} + 1/V_1$ . As a result, we can find  $V_2$  by estimating the slope of this straight line after the  $V_1$  velocity correction.

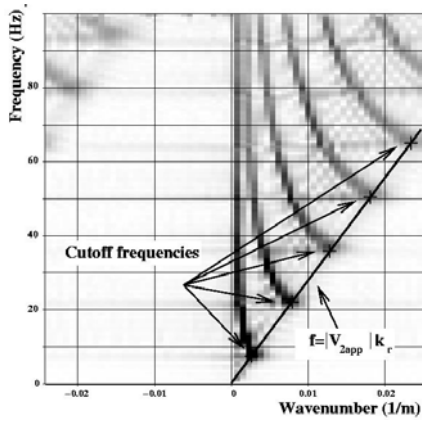


Fig. 5:  $f$ - $k$  representation of the pressure seismogram

### 3.3. Estimation of the water depth

All cutoff frequencies are extracted in term of temporal frequency coordinate. Knowing  $V_1$  and  $V_2$ , equation (2.3) allows us to recover the water depth  $H_1$ .

## 4. APPLICATION ON REAL DATA

Techniques described above are now used on real data to recover geoaoustical parameters. The first example of real data (depth 130 m) was recorded in a simple media which present a flat and horizontal floor along the distance axis. As a result, the depth estimation is very accurate. The two following data (35 and 100 m depths) are more complex because they present a variable depth (a gradient between 90 and 110 m for the “100 m” data) but we show that it is still possible to estimate geoaoustical parameters.

### 5.1. Dataset: depth 130 m

The field data set has been recorded on a synthetic antenna of 240 Ocean Bottom Seismometers (OBS) laid on the North Sea floor. The hydrophone is mainly used but vertical geophone gives identical results for our objective. Spatial sampling and time sampling are 25 m and 4 ms. Initial data are time corrected with velocity  $V_1=1520$  m/s as it was explained in 3.1. Results in time-distance domain and  $f$ - $k$  domain are presented on Fig. 6 and 7. Then,  $V_2$  is estimated using modes: Fig. 7 allows to determine  $V_2=1876$  m/s by following the straight line slope (cf 3.2).

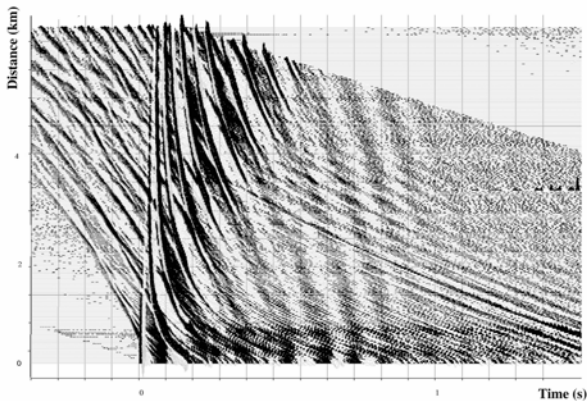


Fig. 6: Pressure seismogram section after  $V_1$  velocity correction

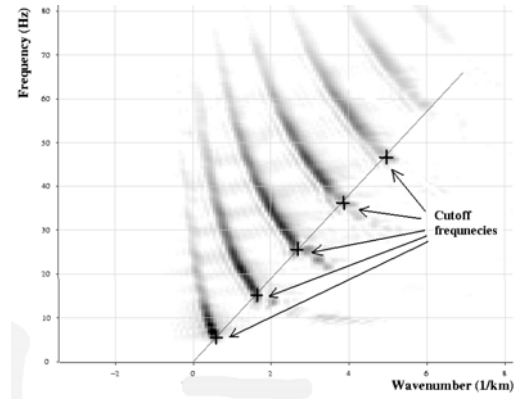


Fig. 7:  $f$ - $k$  representation of the real data section fig. 6

Then, cutoff frequencies of the different modes give several values for the water depth  $H_1$  (eq. 2.3).

Modes	1	2	3	4	5
Freq.(Hz)	6.9	14.7	25.0	35.4	45.0
Depth(m)	94.1	132.4	129.8	128.3	129.8

Estimation of  $H_1$  given by the mode 1 is removed:  $f_{c1}$  is known with a 1 Hz uncertainty which represents 20 %. By averaging, the estimated value of  $H_1$  is then  $H_1=130.1$  m which correspond to the bathymetry (130 m).

### 5.1. Dataset: depth 35 m

We now try to recover geoaoustical parameters on data recorded by 160 OBS with spatial sampling 25 m and time sampling 2 ms. The 4 components: pressure, horizontal (X,Y) and vertical (Z) displacements can be used to recover the geoaoustical parameters. Fig. 8 shows the  $f$ - $k$  representation of the different components after  $V_1$  velocity correction ( $V_1 = 1532$  m/s).

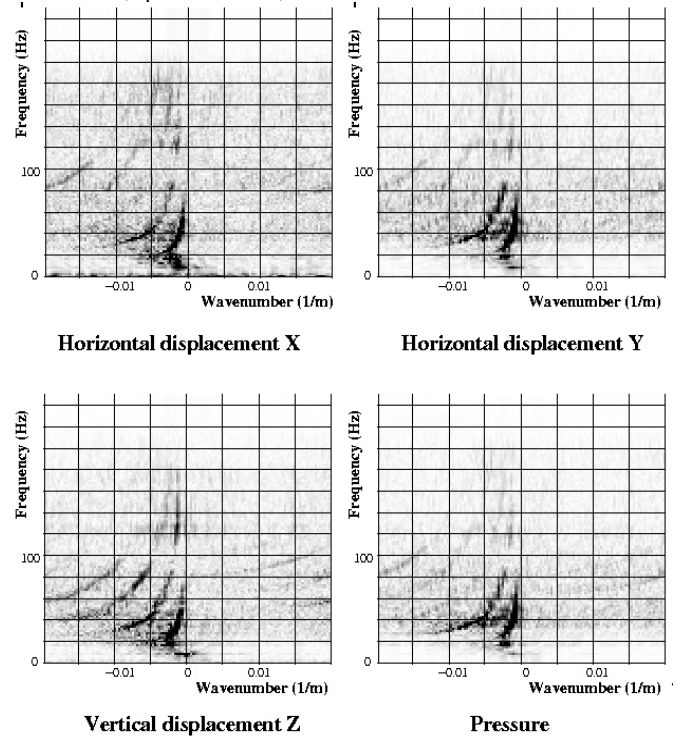


Fig. 8 :  $f$ - $k$  representation of the 3 displacements and of the pressure

On each plot, modes are easily characterized and we identify four straight lines to estimate  $V_2$ . We obtain :

Component	X	Y	Z	Pressure
$V_2$ estimation	2788 m/s	2842 m/s	2709 m/s	2854 m/s

The estimated value of  $V_2$  is the average of the estimations made on the different components:  $V_2=2788$  m/s. The values estimated using different components only differ from the average from 2.8 %. As a result, using four components provides more information and permits a robust and better estimation of  $V_2$ .

As it was done previously,  $H_1$  is estimated with (2.3). We identify two cutoff frequencies related to the two most energetic modes on each representation. Each  $f_{cm}$  give an estimation of  $H_1$ . An average of these eight values is made to obtain the estimation of  $H_1=34.7$  m. This estimation validated by the bathymetry measurement: 35 m.

This data have shown that when the  $f-k$  representation does not permit to identify many cutoff frequencies, it is still possible to estimate the geoacoustical parameters using the four components recorded by an OBS.

### 5.1. Dataset: depth 100 m

The seismic experiment PROSISMA took place in the Gulf of Lyon in 1995. The field data has been recorded by a hydrophone laid on the floor. Total length of the analyzed seismic profile is 14 km. On this portion, water depth varies from 90 m to 110 m which makes the estimation of the water depth more difficult.

Initial data are time corrected with a velocity  $V_1=1520$  m/s as it was explained on the synthetic data in 3.1.  $f-k$  representation of the seismic section is presented on Fig. 9.

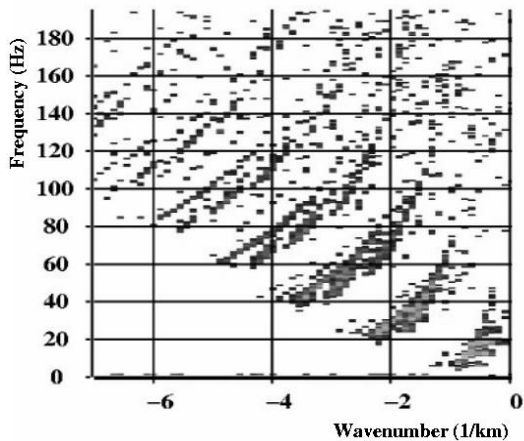


Fig. 9 :  $f-k$  representation of the pressure

Then,  $V_2$  is estimated using modes: Fig. 9 allows to find the straight line slope and so to determine  $V_2=1747$  m/s. Then cutoff frequencies are extracted and  $H_1$  is estimated by averaging the estimations given by the different modes.

Modes	1	2	3	4	5
Freq.(Hz)	6.8	24.4	38.3	57.9	76.5
Depth(m)	113	95	101	93	91

Estimation of  $H_1$  is 99 m which is closed to the bathymetry (from 90 to 110 m). As result, depth estimation is possible even if the seabed is not horizontal (as long as the variations along the distance axis are not to large).

## 10. CONCLUSION

In the Ultra Low Frequency domain and in shallow water configuration, wave propagation is mainly described by guided waves. This type of propagation is well studied in seismic; we have illustrated here that specific methods can be developed to estimate geoacoustical parameters using Ultra Low Frequency waves.

Guided wave propagation has been briefly presented to explain propagation and information carried by these waves. Different transformations (frequency–wavenumber transformation, velocity correction) have been applied to estimate geoacoustical parameters on several real datasets. These data allowed us to validate the proposed method in different environments with different receivers.

## 10. ACKNOWLEDGEMENTS

Authors thank CGG for providing real data set, D. Fattaccioli and J.R. Hartman for their helpful discussions.

## 10. REFERENCES

- [1]K. Aki, P.G. Richards, *Quantitative seismology: theory and methods*, vol. 1, Freeman & Co, U.S.,1980.
- [2]L. Amundsen, A. Reitan, “Estimation of sea-floor wave velocities and density from pressure and particle velocity by AVO analysis”, *Geophysics*, vol. 60, p 1575-1578, 1995.
- [3]N.R. Chapman, C.E. Lindsay, “Matched-field inversion for geoacoustic model parameters in shallow water”, *IEEE Journal of Oceanic Engineering*, vol 21, P 347-354, 1996.
- [4] C.S. Clay, H. Medwin, *Acoustical oceanography: principles and applications*, Willey interscience, Canada, 1977.
- [5] X. Dagany, J.I. Mars and F. Luc, “Multicomponent data analysis and wave separation in marine seismic survey”, 63<sup>rd</sup> Meeting of European Association of Geoscientists and Engineers, Amsterdam, p176, June 2001.
- [6] F. Glangeaud, J.L. Mari, J.L. Lacoume, J. Mars, M. Nardin, “Dispersive seismic waves in geophysics”, *European Journal of Environmental and Engineering Geophysics*, vol. 3, pp 265-306, 1999.
- [7]F.B. Jensen, W.A. Kupperman, M.B. Porter, H. Schmidt, *Computational ocean acoustics*, AIP press, N.Y., 1994.
- [8] M. Nardin, F. Glangeaud and D. Mauuary, “1-200 Hz wave propagation in shallow water”, *Oceans'98, Nice*, 1998.
- [9]B. Nicolas, J. Mars, J-L. Lacoume, D. Fattaccioli, “Are Ultra Low Frequency waves suitable for detection ?”, *Oceans'02, Biloxi*, 2002.
- [10]P. Pignot, « Analyse globale du milieu de propagation pour la tomographie acoustique océanique », PhD Thesis, Grenoble, INPG, 1997.
- [11]Special Issue of *Oceanic Engineering* on “ Inversion Techniques and the variability of sound propagation in shallow water”, vol 21, 1996.